Robotics and Computer–Integrated Manufacturing 51 (2018) 97–102

Contents lists available at ScienceDirect

Robotics and Computer–Integrated Manufacturing

journal homepage: www.elsevier.com/locate/rcim

# Enhancing trajectory tracking accuracy for industrial robot with robust adaptive control

Xiuxing Yin [a,b], Li Pan [b,*]

[a] School of Engineering, University of Warwick, Coventry CV4 7AL, UK
[b] Key Laboratory of E&M, Zhejiang University of Technology, Ministry of Education & Zhejiang Province, Zhejiang, Hangzhou 310014, China

ARTICLE INFO

*Keywords:*
6 DOF industrial robot
Task space
Robust adaptive control
Parametric adaption
Relative tracking errors

ABSTRACT

A robust adaptive control method is systematically proposed in this paper to significantly reduce the relatively tracking errors of 6 degree of freedom (DOF) industrial robots under both external disturbances and parametric uncertainties. The robust adaptive control law is formulated based on the robot dynamics in the task space of the robot end-effector. The control law is designed by combining robust term and adaptive term to track the desired trajectory of the end-effector with sufficient robustness and accuracy in the presence of unknown external disturbances and parametric uncertainties. The trajectory tracking performances of the proposed control are finally guaranteed based on Lyapunov function and Barbalat's lemma. Furthermore, a stable online parametric adaption law is proposed to estimate the unknown parameters in the control law based on persistent excitation and residual estimation. Test results are obtained to show that the combined robust adaptive control reduces the final trajectory tracking error significantly as compared with conventional control.



## 1. Introduction

Industrial robots are base-stationary, reprogrammable and multi-function manipulators that are designed to move material, parts, tools, or specialized devices through variable programmed motions to perform a variety of tasks. The industrial robots have replaced human beings in dangerous, monotonous, or strenuous tasks that humans do not want to do. These activities frequently take place in spaces that are poorly ventilated, poorly lighted, or filled with noxious or toxic fumes. The trend for future industrial robots has been toward the electric-motor powered, servo-controlled industrial robots that are typically floor-standing machines [1]. These industrial robots have proved to be the most cost-effective because they are the most versatile.

As a fundamental and essential subject of industrial robots, the trajectory tracking control has attracted considerable attention over the last few years. A variety of control approaches for high-precision trajectory tracking control of industrial robots have been presented in the literature. The proportional integral derivative (PID) controllers have been widely used for motion tracking control of industrial robots due to the simple structure and model free control design [2]. However, the PID controllers should be carefully tuned according to different operating conditions, which is usually time-consuming. A cooperative target tracking control algorithm was proposed in [3] for motion target tracking of a group of mobile robots. A distributed Kalman filter was also designed to estimate the target position. The effectiveness of the control algorithm was verified based on simulation and experimental results. An adaptive trajectory tracking controller was designed in [4] for robot motion tracking with unknown parameters and uncertain dynamics. The back-stepping controller was designed by using the learning ability of neural networks which avoid the knowledge of the robot dynamics. Simulations and experiments on a commercial robot platform were used to verify the performances of the designed control algorithm with classical back-stepping controller. A model predictive control scheme incorporating neural-dynamic optimization was presented in [5] for robotic trajectory tracking. The model predictive control approach was iteratively transformed as a constrained quadratic programming problem, and then a primal-dual neural network was used to solve this problem over a finite receding horizon. The effectiveness of the control approach was verified based on experiments. A model-free proportional derivative (PD) with sliding mode control law was proposed for robotic trajectory tracking control in [6]. The control law has features of simple linear control provided by PD control and the robust nonlinear control contributed by sliding mode control. However, only simulation results were provided to prove the effectiveness and robustness of the control law. An adaptive back-stepping control scheme was proposed in [7] for trajectory tracking of robot manipulators in the presence of external disturbances and uncertain parameters. The controller was synthesized by using adaptive technique for estimating

* Corresponding author.
*E-mail addresses:* lixingfile@163.com (X. Yin), drevoyage@126.com (L. Pan).

https://doi.org/10.1016/j.rcim.2017.11.007
Received 4 May 2017; Received in revised form 28 October 2017; Accepted 4 November 2017
0736-5845/

robotic system uncertainties. The performances of the controller were verified only based on numerical simulation results. A robust discrete-time sliding mode controller was designed in [8] for trajectory tracking of robotic manipulators by coupling with an uncertainty estimator. The trajectory tracking performances and robustness were evaluated based on experimental results. A decentralized adaptive robust controller was proposed in [9] for trajectory tracking of robot manipulators. A disturbance observer was introduced in each local controller to compensate for the low-passed coupled uncertainties. An adaptive sliding mode control term was also employed to handle the fast-changing components of the uncertainties. However, simulation results were provided to support the theoretical results of the proposed controller. The performance of a fractional order PID controller tuned with evolutionary algorithms was compared in [10] to that with a real coded genetic algorithm in robot trajectory tracking control. The robotic parameters and the given trajectory were changed and white noise was added to test the controllers. Simulation results were provided to show that the controller tuned by PSO performed better than that tuned by the genetic algorithm. Neural networks have also been widely employed for robot trajectory tracking control. In [11], adaptive neural network tracking control for the robotic system with full-state constraints was proposed. The adaptive neural networks were adopted to handle external disturbances and system uncertainties while a Moore-Penrose inverse term was employed to prevent the violation of the full-state constraints. In [12], radial basis function neural network based adaptive impedance controller was developed for robotic motion tracking control with input saturation by considering both uncertainties and input saturation. Extensive simulations were conducted to verify the impedance controller. In [13], a neural network controller was designed for robotic manipulator with input dead-zone by approximating the unknown robotic manipulator dynamics and eliminating the effects of input dead-zone. The feasibility and control performance of the controller were verified based on experiments. In [14], adaptive fuzzy neural network control using impedance learning was designed for a constrained robot with unknown system dynamics. Impedance learning was also introduced to tackle the interaction between the robot and its environment to follow a desired destination generated by impedance learning. The effectiveness of the proposed scheme was illustrated by using some simulation studies.

Even though various control methods have been presented for trajectory control of robots, only a few of them target the motion trajectory control of the six degree of freedom (6DOF) industrial robots. Most of the control methods were designed in the joint angle space of the robots, which may not achieve the final trajectory tracking in the end-effector of the robots. Furthermore, the proposed back-stepping and neural network controllers always necessitate time-consuming and complicated calculations such as repeated partial derivatives, which significantly impede their real-time applications.

Therefore, this paper proposes a systematic method to combine adaptive control and robust control to formulate a robust adaptive control for trajectory tracking of 6 DOF industrial robot under both parametric uncertainties and external disturbances. A stable online parametric adaption law is also proposed to estimate the robot parameters based on persistent excitation. Unlike the existing robot controllers that are primarily designed based on the joint angle spaces, the proposed robust adaptive controller is designed in the task space of the robot's end-effector, which has the potential to significantly enhance the accurate trajectory tracking performances superior to existing controls. The proposed controller also has explicit structure and is easy to implement in industrial robot for real time control due to its relatively lower computational burden as compared with the existing controls in the literature. Furthermore, the proposed control and parametric adaption law are verified based on 6 DOF MITSUBISHI RV-4F industrial robot, which solidly justifies the significantly enhanced control accuracy of the proposed controller.

## 2. Dynamics analysis of industrial robots in the task space

The 6 DOF industrial robots are commonly constituted by 6 moving links coupled by 6 kinematic pairs of the prismatic types. The motion dynamics of the robots can be readily described in the task space of the end-effector [15]. The governing equations of the motion dynamics are usually second-order ordinary differential equations that are useful and required for the real-time feedback control of the robots. Therefore,

$$\mathbf{M}(\mathbf{x})\ddot{\mathbf{x}} + \mathbf{C}(\mathbf{x}, \dot{\mathbf{x}})\dot{\mathbf{x}} + \mathbf{G}(\mathbf{x}) + \mathbf{d} = \mathbf{F} \tag{1}$$

where $\mathbf{M}(\mathbf{x})$ denotes the inertial properties of the robot, $\mathbf{C}(\mathbf{x}, \dot{\mathbf{x}})\dot{\mathbf{x}}$ represents the centrifugal and Coriolis force, $\mathbf{G}(\mathbf{x})$ is the gravitational force, $\mathbf{d}$ represents the effects from un-modeled dynamics and external disturbances, $\mathbf{F}$ denotes the end-effector force vector, which can be designed based on feedback control law, $\mathbf{x}$ is the end-effector position vector in the task space with three rotational and three translational positions.

The parameters of the robot dynamics $\mathbf{M}(\mathbf{x}), \mathbf{C}(\mathbf{x}, \dot{\mathbf{x}})$ and $\mathbf{G}(\mathbf{x})$ in the above equation play a vital role in the control law design of the industrial robot. However, the exact values of these parameters usually cannot be known in advance due to the time-varying working conditions and uncertain environment. The boundaries of these uncertain parameters are generally known or can be calculated priori to implementation.

The forward dynamics of the industrial robot in the task space as described in Eq. (1) can be readily derived from the joint space since each joint angle of the industrial robot can be measureable. For this dynamics equation, the following two properties [16] will be commonly utilized for controller design.

**Property 1.** *$\boldsymbol{M}(\boldsymbol{x})$ is a symmetric and positive definite matrix.*

**Property 2.** *$\dot{\boldsymbol{M}}(\boldsymbol{x}) - 2\boldsymbol{C}(\boldsymbol{x}, \dot{\boldsymbol{x}})$ is a skew-symmetric matrix, i.e. $\boldsymbol{x}^{\boldsymbol{T}}[\dot{\boldsymbol{M}}(\boldsymbol{x}) - 2\boldsymbol{C}(\boldsymbol{x}, \dot{\boldsymbol{x}})]\boldsymbol{x} = 0$.*

The paper aims to synthesize a control law for the input force vector $\mathbf{F}$ to ensure that the position vector of the end-effector $\mathbf{x}$ tracks its desired trajectory $\mathbf{x_d}(t)$ closely while the desired trajectory $\mathbf{x_d}(t)$ is of at least second-order differentiable. The actual control inputs for each joint of the industrial robot can then be calculated from the designed input force vector $\mathbf{F}$ based on inverse dynamics and Jacobin matrix [17].

## 3. Control design

A robust adaptive tracking controller is designed in this section to accurately track the desired trajectory of the end-effector with sufficient robustness and accuracy in the presence of unknown external disturbances and parametric uncertainties.

The tracking error $\mathbf{e}$ of the end-effector can be defined as

$$\mathbf{e} = \mathbf{x_d} - \mathbf{x} \tag{2}$$

A switching manifold $\mathbf{s}$ can thus be defined based on the tracking error as

$$\mathbf{s} = \dot{\mathbf{e}} + \mathbf{\Lambda e} = \left(\dot{\mathbf{x}}_\mathbf{d} + \mathbf{\Lambda e}\right) - \dot{\mathbf{x}} = \dot{\mathbf{x}}_{eq} - \dot{\mathbf{x}} \tag{3}$$

where $\mathbf{\Lambda}$ is a constant positive definite diagonal matrix, $\mathbf{x}_{eq}$ is the equivalent position vector of the end-effector and its orientation with respect to the task space coordinate for specifying an assembly task, $\mathbf{x_d}$ is the desired motion trajectory.

The equivalent position vector of the end-effector can be defined as

$$\dot{\mathbf{x}}_{eq} \triangleq \dot{\mathbf{x}}_\mathbf{d} + \mathbf{\Lambda e} \tag{4}$$

Therefore, the robot dynamics on this manifold can be formulated based on Eq. (1) as

$$\mathbf{M}(\mathbf{x})\dot{\mathbf{s}} = \mathbf{M}(\mathbf{x})\left(\ddot{\mathbf{x}}_{eq} - \ddot{\mathbf{x}}\right) = \mathbf{M}(\mathbf{x})\ddot{\mathbf{x}}_{eq} - \mathbf{F} + \mathbf{C}(\mathbf{x}, \dot{\mathbf{x}})\dot{\mathbf{x}} + \mathbf{G}(\mathbf{x}) + \mathbf{d} \tag{5}$$

In order to design the control law, a positive semidefinite Lyapunov function is defined as

$$\mathbf{V}(t) = \frac{1}{2}\mathbf{s}^\mathbf{T}\mathbf{M}(\mathbf{x})\mathbf{s} \tag{6}$$

Differentiating the Lyapunov function $\mathbf{V}(t)$ with respect to time and noting Property 2 in Section 2 and Eqs. (2)–(5), one obtains

$$\begin{aligned}\dot{\mathbf{V}}(t) &= \frac{1}{2}\mathbf{s}^{\mathbf{T}}\dot{\mathbf{M}}(\mathbf{x})\mathbf{s} + \mathbf{s}^{\mathbf{T}}\mathbf{M}(\mathbf{x})\dot{\mathbf{s}} = \mathbf{s}^{\mathbf{T}}\mathbf{M}(\mathbf{x})\dot{\mathbf{s}} + \mathbf{s}^{\mathbf{T}}\mathbf{C}(\mathbf{x},\dot{\mathbf{x}})\mathbf{s} \\ &= \mathbf{s}^{\mathbf{T}}\left[\mathbf{M}(\mathbf{x})\ddot{\mathbf{x}}_{eq} - \mathbf{F} + \mathbf{C}(\mathbf{x},\dot{\mathbf{x}})\dot{\mathbf{x}}_{eq} + \mathbf{G}(\mathbf{x}) + \mathbf{d}\right] \end{aligned} \tag{7}$$

Based on Eq. (7), the input control force for the end-effector can be defined as

$$\mathbf{F} = \mathbf{F_a} + \mathbf{F_s} \tag{8}$$

where $\mathbf{F_a}$ is a model compensation term and $\mathbf{F_s}$ is a robust control term which consists of two terms $\mathbf{F}_{s1}, \mathbf{F}_{s2}$.

$$\mathbf{F_a} = \hat{\mathbf{M}}(\mathbf{x})\ddot{\mathbf{x}}_{eq} + \hat{\mathbf{C}}(\mathbf{x},\dot{\mathbf{x}})\dot{\mathbf{x}}_{eq} + \hat{\mathbf{G}}(\mathbf{x}) \tag{9}$$

$$\mathbf{F_s} = \mathbf{F}_{s1} + \mathbf{F}_{s2} \tag{10}$$

$$\mathbf{F}_{s1} = \mathbf{K}\mathbf{s} \tag{11}$$

where $\hat{\mathbf{M}}(\mathbf{x})$, $\hat{\mathbf{C}}(\mathbf{x},\dot{\mathbf{x}})$, and $\hat{\mathbf{G}}(\mathbf{x})$ are estimates of the matrices $\mathbf{M}(\mathbf{x})$, $\mathbf{C}(\mathbf{x},\dot{\mathbf{x}})$ and $\mathbf{G}(\mathbf{x})$, respectively, $\mathbf{F}_{s1}$ and $\mathbf{F}_{s2}$ are respectively a feedback term for stabilization and a robust term for eliminating the effects from external disturbances and parametric uncertainties, and $\mathbf{F}_{s2}$ is to be determined in the following, $\mathbf{K}$ is a symmetric positive definite matrix.

The parametric uncertainties can be described as

$$\begin{cases} \tilde{\mathbf{M}}(\mathbf{x}) = M(\mathbf{x}) - \hat{\mathbf{M}}(\mathbf{x}) \\ \tilde{\mathbf{C}}(\mathbf{x},\dot{\mathbf{x}}) = C(\mathbf{x},\dot{\mathbf{x}}) - \hat{\mathbf{C}}(\mathbf{x},\dot{\mathbf{x}}) \\ \tilde{\mathbf{G}}(\mathbf{x}) = G(\mathbf{x}) - \hat{\mathbf{G}}(\mathbf{x}) \end{cases} \tag{12}$$

where $\tilde{\mathbf{M}}(\mathbf{x})$, $\tilde{\mathbf{C}}(\mathbf{x},\dot{\mathbf{x}})$ and $\tilde{\mathbf{G}}(\mathbf{x})$ denote the parametric variations of the respective matrices.

Substituting Eqs. (8)–(11) into Eq. (7) yields

$$\dot{\mathbf{V}}(t) = -\mathbf{s}^{\mathbf{T}}\mathbf{K}\mathbf{s} + \mathbf{s}^{\mathbf{T}}\left[\tilde{\mathbf{M}}(\mathbf{x})\ddot{\mathbf{x}}_{eq} + \tilde{\mathbf{C}}(\mathbf{x},\dot{\mathbf{x}})\dot{\mathbf{x}}_{eq} + \tilde{\mathbf{G}}(\mathbf{x}) + \mathbf{d} - \mathbf{F}_{s2}\right] \tag{13}$$

The robust term $\mathbf{F}_{s2}$ can be designed so that the closed robot control system can be stabilized. Thus,

$$\mathbf{F}_{s2} = \beta(\Delta + \eta)\mathbf{sgn}(\mathbf{s}) \tag{14}$$

where $\beta$, $\Delta$ and $\eta$ are positive definite coefficients, respectively.

$$\begin{cases} \beta \geq 1 \\ \Delta \geq \left\|\tilde{\mathbf{M}}(\mathbf{x})\right\|\left\|\ddot{\mathbf{x}}_{eq}\right\| + \left\|\tilde{\mathbf{C}}(\mathbf{x},\dot{\mathbf{x}})\right\|\left\|\dot{\mathbf{x}}_{eq}\right\| \\ \qquad + \left\|\tilde{\mathbf{G}}(\mathbf{x})\right\| + \|\mathbf{d}\| \end{cases} \tag{15}$$

Substituting Eq. (14) into Eq. (13) yields

$$\dot{\mathbf{V}}(t) = -\mathbf{s}^{\mathbf{T}}\mathbf{K}\mathbf{s} - \mathbf{s}^{\mathbf{T}}\mathbf{sgn}(\mathbf{s})\left[\begin{array}{c} \beta(\Delta+\eta)- \\ \left(\tilde{\mathbf{M}}(\mathbf{x})\ddot{\mathbf{x}}_{eq} + \tilde{\mathbf{C}}(\mathbf{x},\dot{\mathbf{x}})\dot{\mathbf{x}}_{eq} + \right. \\ \left.\tilde{\mathbf{G}}(\mathbf{x}) + \mathbf{d}\right)\mathbf{sgn}(\mathbf{s}) \end{array}\right] \tag{16}$$

By considering Eq. (15), Eq. (16) can be re-written as

$$\dot{\mathbf{V}}(t) = -\mathbf{s}^{\mathbf{T}}\mathbf{K}\mathbf{s} - \eta\|\mathbf{s}\| \leq 0 \tag{17}$$

As demonstrated in (17), the closed robot control system can be stabilized by using the robust adaptive control law Eqs. (8)–(11) and all the signals will be bounded in spite of unknown external disturbances and parametric uncertainties. Also, the final zero trajectory tracking error of the end-effector can be eventually guaranteed at steady-state based on Barbalat's lemma [18]. Therefore, $\mathbf{x} \to \mathbf{x_d}$ as $t \to \infty$.

## 4. Parametric adaptions

In practice, the parametric estimates $\hat{\mathbf{M}}(\mathbf{x})$, $\hat{\mathbf{C}}(\mathbf{x},\dot{\mathbf{x}})$, and $\hat{\mathbf{G}}(\mathbf{x})$ are essentially needed in the above robust adaptive tracking control design for the industrial robot. Therefore, a stable online parametric adaption law is proposed to estimate these parameters in real time based on persistent excitation.

The robot dynamics Eq. (1) can be re-written as a linear regression model. Thus,

$$\mathbf{F} = \boldsymbol{\gamma}^{\mathbf{T}}\boldsymbol{\vartheta} \tag{18}$$

where the vectors $\boldsymbol{\gamma}$ and $\boldsymbol{\vartheta}$ can be respectively described as

$$\boldsymbol{\gamma}^{\mathbf{T}} = \left[\ddot{\mathbf{x}}, \dot{\mathbf{x}}, \mathbf{I}\right]; \boldsymbol{\vartheta} = \left[\mathbf{M}(\mathbf{x}), \mathbf{C}(\mathbf{x},\dot{\mathbf{x}}), \mathbf{G}(\mathbf{x})\right]^{\mathbf{T}} \tag{19}$$

A pre-filter $\mathbf{H}_f$ is designed and applied to both sides of Eq. (18) to eliminate possible high-frequency measurement noises. Thus, the transfer function of this pre-filter can be described as

$$\mathbf{H_f} = \frac{1}{s\omega_f + 1} \tag{20}$$

where $\omega_f$ is the cut-off frequency of this filter and $s$ is the Laplace operator.

By applying the pre-filter in Eq. (20) to both sides of Eq. (19), the filtered robot dynamics can be re-arranged as

$$\mathbf{F}_f = \boldsymbol{\gamma}_f^{\mathbf{T}}\boldsymbol{\vartheta} \tag{21}$$

where $\boldsymbol{\gamma}_f^{\mathbf{T}} = [\ddot{\mathbf{x}}_f, \dot{\mathbf{x}}_f, \mathbf{I}_f]$ is the filtered velocity and acceleration vector of the end-effector, $\mathbf{F}_f$ is the filtered end-effector force vector.

The parameter vector $\boldsymbol{\vartheta}$ can be reasonably estimated online based on the least square estimation algorithm with best parameter estimation convergence [19]. In order to use the least square estimation algorithm for parametric estimation, the end-effector force estimation error can be defined as

$$\boldsymbol{\xi} = \hat{\mathbf{F}}_f - \mathbf{F}_f = \boldsymbol{\gamma}_f^{\mathbf{T}}\hat{\boldsymbol{\vartheta}} - \mathbf{F}_f \tag{22}$$

The following adaptation function $\boldsymbol{\tau}$ is designed for the estimation of parameter vector $\boldsymbol{\vartheta}$ [20]:

$$\boldsymbol{\tau} = \frac{-\boldsymbol{\gamma}_f\boldsymbol{\xi}}{1 + \boldsymbol{\alpha}\mathbf{tr}\left\{\boldsymbol{\gamma}_f^{\mathbf{T}}\boldsymbol{\Gamma}\boldsymbol{\gamma}_f\right\}} \tag{23}$$

where $\alpha$ and $\boldsymbol{\Gamma}$ denote a forgetting factor and a covariance matrix, respectively.

The covariance matrix $\boldsymbol{\Gamma}$ can be described as

$$\dot{\boldsymbol{\Gamma}} = \begin{cases} \boldsymbol{k}\boldsymbol{\Gamma} - \frac{\boldsymbol{\Gamma}\boldsymbol{\gamma}_f\boldsymbol{\gamma}_f^{\mathbf{T}}\boldsymbol{\Gamma}}{1+\boldsymbol{\alpha}\mathbf{tr}\left\{\boldsymbol{\gamma}_f^{\mathbf{T}}\boldsymbol{\Gamma}\boldsymbol{\gamma}_f\right\}} & \text{if } \boldsymbol{\lambda}_{max}(\boldsymbol{\Gamma}) \leq \rho_{\mathrm{m}} \\ \mathbf{0} & \text{otherwise} \end{cases} \tag{24}$$

where $\lambda_{max}(\boldsymbol{\Gamma})$ is the maximum eigenvalue of the matrix $\boldsymbol{\Gamma}$, and $\rho_m$ is the preset upper bound for the eigenvalue.

Therefore, a projection-type parametric adaptation law can be established as

$$\frac{\mathrm{d}\boldsymbol{\vartheta}}{\mathrm{dt}} = \mathbf{proj}_{\hat{\boldsymbol{\vartheta}}_f}(\boldsymbol{\Gamma}\boldsymbol{\tau}) = \begin{cases} 0 & \text{if } \hat{\boldsymbol{\vartheta}} = \boldsymbol{\vartheta}_{max} \\ 0 & \text{if } \hat{\boldsymbol{\vartheta}} = \boldsymbol{\vartheta}_{min} \\ \boldsymbol{\Gamma}\tau & \text{otherwise} \end{cases} \tag{25}$$

where $\boldsymbol{\vartheta}_{max}$ and $\boldsymbol{\vartheta}_{min}$ denote the maximum and minimum values of the parameter vector $\boldsymbol{\vartheta}$.

With the parametric adaptation law in Eq. (25) and the least-squares-type estimation function, the estimate of the parameter vector $\hat{\boldsymbol{\vartheta}}$ converges to the real value $\boldsymbol{\vartheta}$ in finite time, i.e., $\tilde{\boldsymbol{\vartheta}} \to 0$ as $t \to \infty$, if the following persistent excitation condition [21] is satisfied

$$\int_{\mathbf{t}}^{\mathbf{t}+\mathbf{T}} \boldsymbol{\gamma}_f\boldsymbol{\gamma}_f^{\mathbf{T}}\mathbf{d}\boldsymbol{\chi} \geq \mathbf{k_p}\mathbf{I_p} \tag{26}$$

where $\boldsymbol{k}_p$ and $\mathbf{I}_p$ denote respectively certain constant matrix and certain unit matrix that can be reasonably selected.

When the parameter vector $\boldsymbol{\vartheta}$ is updated by the parametric adaptation law with the persistent excitation condition, the designed robust

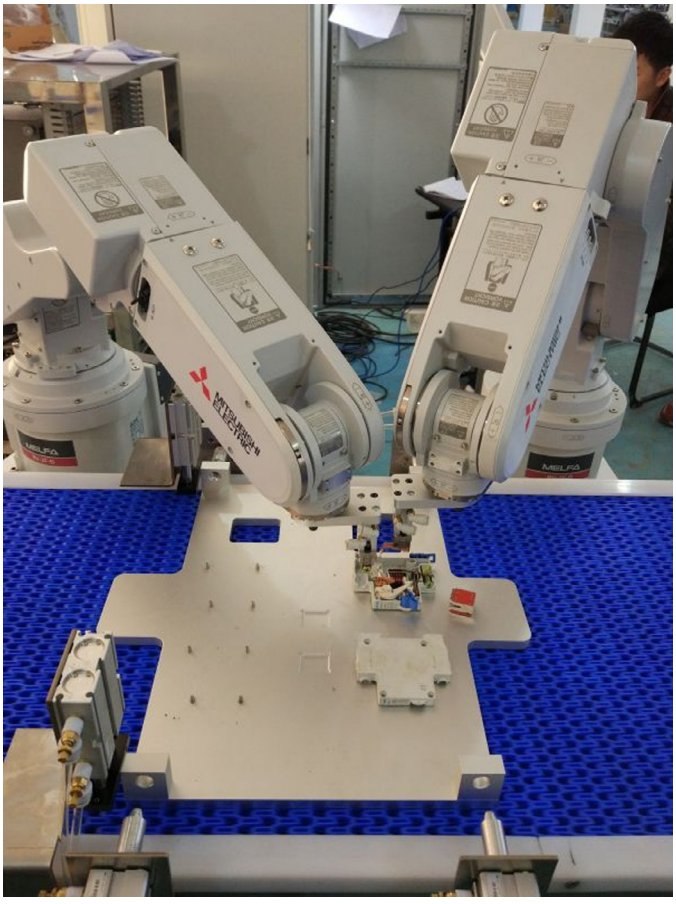

**Fig. 1.** Experimental platform of 6 DOF assembly industrial robots.

adaptive control law will guarantee that the closed-loop robotic control system will be asymptotically stable and the steady state tracking error will eventually converge to zero in finite time regardless of unknown external disturbances and parametric uncertainties.

## 5. Verifications and discussions

Comparative test results have been obtained to verify the effectiveness of the robust adaptive control law and the parametric adaption law. Fig. 1 shows the experimental setup of the dual 6 DOF MITSUBISHI RV-4F industrial robotic system, which can be mainly employed to assemble low voltage electric components made of soft materials, such as electrical air switches. The maximum payload, the maximum operating speed and the position repeatability accuracy of the dual robots are respectively 4 kg, 9 m/s and 0.02 mm. The joints of the robotic system are all driven by 400 W AC servo motors with position encoders that can provide necessary information, such as joint angular displacements, for feedback control. Other parameters in the control design and parametric adaptions can be readily derived based on measured signals.

One industrial robot is used for the implementations of the control law and parametric adaption law during part assembling tasks while the other robot is used as the external disturbances in the assembling process. The external disturbances in the control implementations also arise from the effects of the material compliance such as elasticity since soft electrical materials are manipulated, which will bring in additional uncertainties.

The tests have been conducted for three times based on typical part assembling procedure. The robot was first commanded to pick up an assembling object from an initial point, lift and hold the object for several seconds, and then place the object into an assembling hole to finish the task. After finishing the assembling task, the robot will return to the initial point to continue and repeat the next assembling motion. The desired motion trajectory programming was synthesized in the Cartesian space with a fixed tool orientation and the desired trajectory consists of several straight lines connected with each other for completing the assembling task. Although the employed industrial robot has six DOF, only 3 DOF are actually used during the experiments since the axis of the robot wrist coincides with that of the assembling hole and the robot arm is fixed on the ground where the control system is placed.

**Table 1**
Major parameters of the tests.

| Parameter | Value | Nomenclature |
|---|---|---|
| $\Lambda$ | diag{1.8, 1.2, 1.6, 2.1, 2.2, 3.4} | The constant positive definite diagonal matrix |
| $K$ | diag{16, 19, 26, 43, 68, 89} | The symmetric positive definite matrix |
| $\beta$ | 1.2 | The positive definite gain |
| $\Delta$ | 1269 | The boundary coefficient |
| $\eta$ | 28 | The positive definite gain |
| $\omega_f$ | 20 Hz | The cut-off frequency |
| $\alpha$ | 0.4 | Forgetting factor |
| $\Phi$ | 0.9 | The boundary layer thickness |

The proposed control and parametric adaption laws have been simulated in MATLAB Robotics Toolbox based on the experimental data. The actual force for parametric estimations can be measured from a load cell mounted on the end-effector of the industrial robot, while the applied control force can be analyzed and calculated based on the robust adaptive control law in Eqs. (8)–(11). The control performances of the proposed control have also been compared with a proportional derivative (PD) controller under the same operating conditions [22]. The tests have been repeated for more than 10 times and the test data have been averaged over a long time to obtain relatively stable tracking results.

In practice, the signum function sgn(s) in Eq. (14) may lead to significant chattering problem due to measurement noises. The chattering effects can be eliminated by replacing a signum function with a saturation function with the boundary layer thickness $\Phi$ [23]. Thus, the boundary layer thickness $\Phi$ can be tuned to control the amount of chattering. Thus,

$$\mathbf{sat}\left(\frac{\mathbf{s}}{\Phi}\right) = \begin{cases} \frac{\mathbf{s}}{\Phi} & \text{if } \left|\frac{\mathbf{s}}{\Phi}\right| < 1 \\ \mathbf{sgn}\left(\frac{\mathbf{s}}{\Phi}\right) & \text{otherwise} \end{cases} \tag{28}$$

The main parameters of the proposed tracking control and parametric adaption law are tabulated in Table. 1. The initial positions of the joints and end-effector are reset as $\dot{\mathbf{x}} = \dot{\boldsymbol{\theta}} = [0,\ 0, 0, 0, 0, 0]^{\mathrm{T}}, \mathbf{x} = \boldsymbol{\theta} = [0,\ 0, 0, 0, 0, 0]^{\mathrm{T}}$ when starting the experiments.

In order to evaluate the performances of the two controllers, the following metrics are formulated as follows:

(a) The averaged relative tracking error for the robotic joint angles

$$\frac{1}{6\mathrm{N}} \sum_{i=1}^{6} \sum_{j=1}^{\mathrm{N}} \frac{\theta_{dij} - \theta_{ij}}{\theta_{dij}} \times 100\% \tag{29}$$

where $\theta_{ij}$ and $\theta_{dij}$ denote the jth sampling data of the ith element of the joint angle trajectory $\theta$ and reference trajectory vector $\theta_d$, respectively, N denotes the number of sampling data.

(b) The averaged relative tracking error of the robot end-effector

$$\frac{1}{6\mathrm{N}} \sum_{i=1}^{6} \sum_{j=1}^{\mathrm{N}} \frac{\mathbf{x}_{dij} - \mathbf{x}_{ij}}{\mathbf{x}_{dij}} \times 100\% \tag{30}$$

where $\mathbf{x}_{ij}$ and $\mathbf{x}_{dij}$ denote the jth sampling data of the ith element of the end-effector's trajectory vector $\mathbf{x}$ and reference trajectory vector $\mathbf{x_d}$, respectively.

**Table 2**
The RAEs of the joint torque estimations based on parametric adaptions.

| Tests | Joint 1 | Joint 2 | Joint 3 | Joint 4 | Joint 5 | Joint 6 |
|---|---|---|---|---|---|---|
| 1 | 0.0186 | 0.0528 | 0.0340 | 0.0458 | 0.0782 | 0.0926 |
| 2 | 0.0343 | 0.0628 | 0.0453 | 0.0621 | 0.0829 | 0.0965 |
| 3 | 0.0518 | 0.0689 | 0.0520 | 0.0682 | 0.0786 | 0.0826 |
| Means | 0.0349 | 0.0615 | 0.0438 | 0.0587 | 0.0799 | 0.0906 |

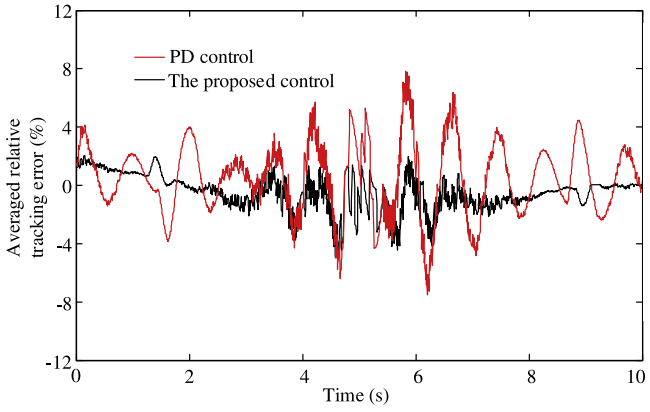


**Fig. 2.** The averaged relative tracking errors of the joint angles based on the two controls.

(c) The normalized average control signals of the joints

$$\frac{1}{6N}\sum_{i=1}^{6}\sum_{j=1}^{N}\frac{u_{ij}}{u_{ijmax}} \times 100\% \tag{31}$$

where $u_{ij}$ and $u_{ijmax}$ denote the jth sampling data of the ith element of the joint control signals and the maximum control signals. The maximum value of the control signals is 12 V.

(d) The normalized averaged estimates of the uncertain parameters of the robot can be formulated as

$$\frac{1}{18N}\sum_{i=1}^{3}\sum_{j=1}^{N}\sum_{k=1}^{6}\frac{\hat{Y}_{ijk}}{Y_{ijkmax}} \times 100\% \tag{32}$$

where $\hat{Y}_{ijk}$ and $Y_{ijkmax}$ denote the kth element value, jth sampling data of the ith element of the estimate vectors and the maximum values of the parametric vectors, respectively.

(e) The relative absolute error (RAE) of the joint torque estimations based on parametric adaptions is also defined and measured in three tests to evaluate the accuracy of the proposed parametric adaption method [24]. Thus,

$$\frac{\sum_{k=1}^{3}\left|\tau_{est\_k}-\tau_k^*\right|}{\sum_{k=1}^{3}\left|\tau_k^*-\overline{\tau_k^*}\right|} \tag{33}$$

where k denotes the number of the tests, $\tau_{est\_k}$ is the estimated joint torque based on the proposed parametric adaption method in the kth test, $\tau_k^*$ is the measured torque in the kth test, $\overline{\tau_k^*}$ is the average of $\tau_k^*$. Table 2 summarizes the RAEs of the joint torque estimations based on parametric adaptions. As illustrated in this table, the RAEs of the joint torques can be reasonably maintained within [0.03, 0.10], which is relatively accurate for estimating the joint torques and robotic parameters. Therefore, the proposed parametric adaption method can be utilized to estimate the robotic parameters with relatively high accuracy.

As described in Figs. 2 and 3, the relative tracking errors of both the joint angles and end-effector oscillate significantly between −8% and 8% by using PD control, while the relative tracking errors can be significantly reduced within −4% and 4% when the proposed control law is applied. The relative tracking errors of both the two controls increase considerably when an external disturbance from the robot collision was added at around 4 s. However, the relative tracking errors can

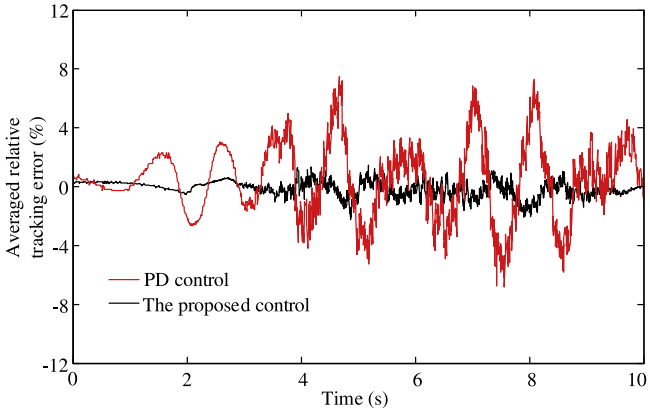


**Fig. 3.** The averaged relative tracking errors of the end-effector based on two controls.

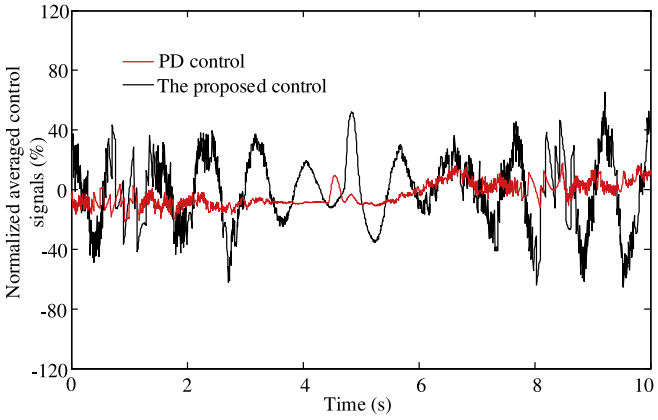


**Fig. 4.** The normalized average control signals of the joints based on two controls.

be quickly maintained at relatively lower value by using the proposed control, while the relative tracking errors cannot be quickly reduced and are still relatively high by using the conventional PD control. The control effects after the disturbance input indicate the robustness of the proposed control in stabilizing and reducing the relative tracking errors with relatively less response time as compared with the conventional PD control. Therefore, the proposed control is capable of maintaining relatively higher trajectory tracking accuracy and reducing the induced tracking errors by external disturbances with fast responses when compared with the conventional PD control.

As illustrated in Fig. 4, the normalized average control signals from the proposed robust adaptive control law are relatively higher than that from the conventional PD control. The control signals of the proposed controller also increase after the external disturbances, which indicates that the proposed control exerts more efforts to reduce the increased tracking errors induced from external disturbances. The facts demonstrate that the proposed control is more active in maintaining the desired tracking trajectory by reducing the relative tracking errors with fast responses as compared with the conventional PD control.

Fig. 5 illustrates the normalized average robot parametric estimates based on the proposed parametric adaption law, which converge eventually to their stable values in finite time as the relative tracking errors converge to zero. This demonstrates the proposed parametric adaptation law can be readily employed in the control implementations for estimating unknown parameters. The control design and implementations can be achieved without considering specific values of these parameters since these parameters can be quickly estimated online along with the control implementation process.

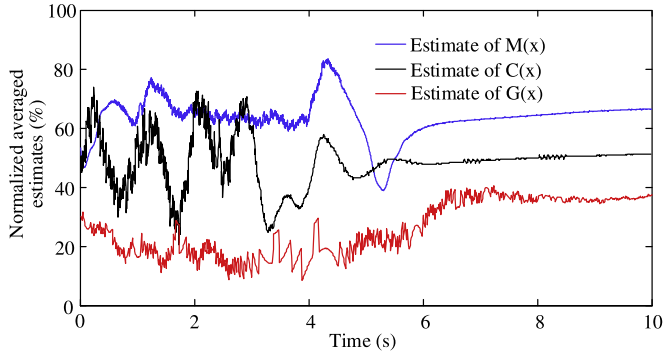


**Fig. 5.** The normalized average robot parametric estimates based on the proposed parametric adaption law.

## 5. Conclusion

This paper has presented the robust adaptive control for trajectory tracking control of a 6 DOF industrial robot in the task space of the end-effector regardless of parametric variations and uncertain disturbances. Furthermore, the stable online parametric adaption law has been proposed to estimate the robot parameters in real time based on persistent excitation. The transient and stable performances of the proposed control law have been verified through Lyapunov function. By combining the robust and adaptive terms to enhance the tracking accuracy, the proposed robust adaptive control preserves the advantages of both the robust and adaptive controls while eliminating their drawbacks. Test results have also been obtained to show that the proposed control achieves the guaranteed transient and steady-state performance regardless of the estimation errors and external disturbances and the final trajectory errors can be significantly reduced by using the proposed controller as compared to the conventional PD control method. With the significant improvements in the tracking accuracy and stability of the industrial robot, the proposed controller is well positioned to be widely used in the control of industrial robots, especially in the autonomous assembly operations.

## References

[1] Z. Pan, J. Polden, N. Larkin, et al., Recent progress on programming methods for industrial robots, Rob. Comput. Integr. Manuf. 28 (2) (2012) 87–94.
[2] H.V.H. Ayala, L. dos Santos Coelho, Tuning of PID controller based on a multi-objective genetic algorithm applied to a robotic manipulator, Expert Syst. Appl. 39 (10) (2012) 8968–8974.
[3] Z. Wang, D. Gu, Cooperative target tracking control of multiple robots, IEEE Trans. Ind. Electron. 59 (8) (2012) 3232–3240.
[4] O. Mohareri, R. Dhaouadi, A.B. Rad, Indirect adaptive tracking control of a nonholonomic mobile robot via neural networks, Neurocomputing 88 (2012) 54–66.
[5] Z. Li, J. Deng, R. Lu, et al., Trajectory-tracking control of mobile robot systems incorporating neural-dynamic optimized model predictive approach, IEEE Trans. Syst. Man Cybern. 46 (6) (2016) 740–749.
[6] P.R. Ouyang, J. Acob, V. Pano, PD with sliding mode control for trajectory tracking of robotic system, Rob. Comput. Integr. Manuf. 30 (2) (2014) 189–200.
[7] Q. Hu, L. Xu, A. Zhang, Adaptive backstepping trajectory tracking control of robot manipulator, J. Franklin Inst. 349 (3) (2012) 1087–1105.
[8] M.L. Corradini, V. Fossi, A. Giantomassi, et al., Discrete time sliding mode control of robotic manipulators: development and experimental validation, Control Eng. Pract. 20 (8) (2012) 816–822.
[9] Z.J. Yang, Y. Fukushima, P. Qin, Decentralized adaptive robust control of robot manipulators using disturbance observers, IEEE Trans. Control Syst. Technol. 20 (5) (2012) 1357–1365.
[10] Z. BİNGÜL, O. KARAHAN, Fractional PID controllers tuned by evolutionary algorithms for robot trajectory control, Turk. J. Electr. Eng. Comput. Sci. 20 (Sup. 1) (2012) 1123–1136.
[11] H. Wei, Y. Chen, Z. Yin, Adaptive neural network control of an uncertain robot with full-state constraints, IEEE Trans. Cybern. 46 (3) (2016) 620–629.
[12] H. Wei, Y. Dong, C. Sun, Adaptive neural impedance control of a robotic manipulator with input saturation, IEEE Trans. Syst. Man Cybern. 46 (3) (2016) 334–344.
[13] H. Wei, Y. Ouyang, J. Hong, Vibration control of a flexible robotic manipulator in the presence of input deadzone, IEEE Trans. Ind. Inf. 13 (1) (2017) 48–59.
[14] H. Wei, Y. Dong, Adaptive fuzzy neural network control for a constrained robot using impedance learning, IEEE Trans. Neural Netw. Learn. Syst. (2017) 99.
[15] B. Siciliano, L. Sciavicco, L. Villani, G. Oriolo, Robotics: Modelling, Planning and Control, Springer Science & Business Media, August 20, 2010.
[16] J.J. Craig, Introduction to Robotics: Mechanics and Control, Pearson Prentice Hall, Upper Saddle River, 2005.
[17] R.M. Murray, et al., A Mathematical Introduction to Robotic Manipulation, CRC press, 1994.
[18] J.J.E. Slotine, W. Li, Applied Nonlinear Control, Prentice Hall, NJ: Englewood Cliffs, 1991.
[19] I.D. Landau, R. Lozano, M. M'Saad, Adaptive Control, Springer-Verlag, NewYork, 1998.
[20] B. Yao, Integrated direct/indirect adaptive robust control of SISO nonlinear systems in semi-strict feedback form, in: Proc. Amer. Control Conf., Denver, CO, 2003, pp. 3020–3025.
[21] E. Žáčeková, S. Prívara, M. Pčolka, Persistent excitation condition within the dual control framework, J. Process Control 23 (9) (2013) 1270–1280.
[22] Y.X. Su, P.C. Müller, C.H. Zheng, Global asymptotic saturated PID control for robot manipulators, IEEE Trans. Control Syst. Technol. 18 (6) (2010) 1280–1288.
[23] J. Kim, S.B. Choi, Design and modeling of a clutch actuator system with self-energizing mechanism, IEEE/ASME Trans. Mechatron. 16 (5) (2011) 953–966.
[24] Z. Bingül, O. Karahan, Dynamic identification of Staubli RX-60 robot using PSO and LS methods, Expert Syst. Appl. 38 (2011) 4136–4149.